Ultrasonics 99 (2019) 105962

Contents lists available at ScienceDirect

Ultrasonics

journal homepage: www.elsevier.com/locate/ultras

Use of acoustic emission to evaluate the micro-mechanical behavior of sands in single particle compression tests

Wenli Lin[a,*], Ang Liu[b], Wuwei Mao[c]

[a] Department of Civil Engineering, The University of Tokyo, Tokyo 113-8656, Japan
[b] Department of Geological Engineering, Nanjing Tech University, Nanjing 211800, China
[c] Department of Geotechnical Engineering, College of Civil Engineering, Tongji University, Shanghai 200092, China

ARTICLE INFO

Keywords:
Acoustic Emission (AE)
Micro-mechanical behavior
Sandy particle
AE hit rate
Frequency characteristic
Microcracking

ABSTRACT

Particle breakage has been recognized as a crucial factor affecting the mechanical behavior of stressed granular assemblages. To understand such underlying micro-mechanical behavior, Acoustic Emission (AE) technique that is capable of continuously diagnosing the deterioration and failure process of stressed materials was employed into single particle compression tests on silica sands. Regardless of different particle sizes, the fracturing process could be highly featured by AE characteristics, in which AE hit rate and peak frequency characteristics were analyzed to evaluate the intensity and mode of micro-mechanical behaviors, respectively. “Early warning omens” regarding the impending failure of the stressed particle is revealed in terms of the initiation and rapid increase of high-frequency AE components, as well as the rapid increase of AE hit rate. The effect of “prehistory of failure” on the stressed particle is sensitively featured by the highly emitted AE events after the catastrophic failure. Furthermore, a frequency-based method is suggested to distinguish different modes of micro-mechanical behaviors associated with particle readjustment, asperity abrasion, and microcracking. Further employment of the present result is expected to continuously evaluate the intensity and mode of particle interactions in stressed granular assemblages.

1. Introduction

Particle breakage has been recognized as a crucial factor affecting the mechanical behavior of stressed granular assemblages, e.g. decreasing the permeability and friction angle, changing critical state line locations and suppressing the dilatancy behavior, etc. [1–3]. To understand the underlying micro-mechanical behavior of particle breakage and correlate it with the strength parameter of granular assemblages, single-particle compression test incorporating with new advanced technologies is commonly adopted and has been extensively performed for various particle sizes and mineral types [4–7]. However, previous studies and involved techniques focused on either boundary measurement (e.g. high-speed microscope camera) or local density detection with a wide measurement time interval (e.g. X-ray micro-computed tomography), which could hardly evaluate the intensity and mode of micro-mechanical behaviors continuously within an individual particle subjected to compression.

As a non-destructive testing method, Acoustic Emission (AE) technique is capable of continuously capturing released elastic waves inside a stressed material. It has been widely used in quasi-continuum materials including metal, rock and concrete, etc. When the material is under stress, the micro-scale deterioration, such as cracking in rock and concrete, is accompanied by a sudden release of stored strain energy in the typical form of elastic waves. Such elastic waves could be detected by AE sensors and recorded as acoustic emissions [8]. Previous researches have reported that interpreting the information carried by AE waveforms (e.g. signal arrival time, AE hit rate, AE frequency, etc.) could pinpoint the location of deterioration [9–11], diagnose the intensity of failure [12,13], and distinguish the mode of associated micro-mechanical behaviors [14–16], etc.

Particle fragmentation associated micro-mechanical behaviors (in terms of particle adjustment, asperity abrasion, and microcracking, etc.) would also generate AE activities. The interpretation of AE activities might, hence, provide beneficial information in understanding the micro-mechanical behavior of granular assemblages. To date, the application of AE technique in granular materials is still marginal due to the intrinsic propagation complexity of acoustic waves in discrete materials. Nevertheless, a few instructive observations have recently shown a promising correlation between AE characteristics and the underlying micro-mechanical behavior of granular materials. For instance,

* Corresponding author.
E-mail address: lwlcsu@geot.t.u-tokyo.ac.jp (W. Lin).

https://doi.org/10.1016/j.ultras.2019.105962
Received 16 December 2018; Received in revised form 10 July 2019; Accepted 12 July 2019
Available online 13 July 2019
0041-624X/

Table 1
Details of particles involved in single particle compression tests.

Testing item	Test number	Material component	Averaged particle size (mm)	Illustration
Silica # 1	10	Siliceous	6.79 × 5.36 × 4.53	Fig. 1 (a)
Silica # 2	10	Siliceous	4.61 × 4.26 × 3.62	Fig. 1 (b)
Silica # 3	10	Siliceous	3.57 × 3.26 × 2.50	Fig. 1 (c)
Silica # 4	10	Siliceous	2.95 × 2.46 × 2.06	Fig. 1 (d)
Silica # 5	10	Siliceous	2.18 × 1.85 × 1.53	Fig. 1 (e)

regarding AE hit rate, Dixon et al. [17] and Smith et al. [18] established a linear relationship between AE hit rate and displacement rate, which was then used to provide early warning for the instability of soil slopes. Regarding AE frequency response, the second author found that the fragmentation of sandy particles is accompanied by a significant rising of high-frequency AE components (> 100 kHz) regardless of different mineral components, while particle-to-particle sliding behavior is dominant with low-frequency components [16]. More recently, Luo et al. [19,20] and Ibraim et al. [21] conducted plenty of single particle compression tests and stated that AE characteristics could characterize the crushing mechanism and signature. However, only limited AE signals generated during the crushing period were extracted for analysis.

This paper attempts to understand the effect of particle sizes on the micro-mechanical behavior of single particle breakage and on the characteristics of AEs. To this end, single particle compression tests combined with AE technique were conducted on silica sand particles with various sizes under dry condition. The mechanical behavior of sand particles and the corresponding AE characteristics (in terms of AE hit rate and peak frequency) were analyzed, and the potential usage of AE characteristics in continuously evaluating the intensity and mode of micro-mechanical behaviors in granular sands were explored.

2. Testing preparation

2.1. Testing material and apparatus

Silica sands, which have been widely used in laboratory experiments in Japan, were selected as the testing material in this work. Sand particles with five different sizes (as illustrated in Table 1) were selected to conduct the single particle compression test under dry condition. 10 tests were conducted for each size of the particle, and 50 tests in total were conducted for all particles. The optical images in Fig. 1 show the particles selected for testing, in which larger particles have a higher degree of roundness and a relatively smoother surface with successions of pre-existed micro-defects, while smaller particles are more angular and rougher with successions of asperities on their surfaces.

A conventional servo-controlled loading apparatus, with loading rates ranged from 0.001 to 2.5 mm/min, was used to conduct single particle compression tests. During testing, a steel cylinder was fixed above the bottom pedestal (Fig. 2 (a)) and acted as the bottom loading platen, while the top cap of the apparatus acted as the top loading platen. Both the surfaces of the loading platens were fully polished to reduce friction. Two noise barriers (as shown in Fig. 2 (b) and Fig. 2(c)), made by attaching several layers of thin metal plates and latex membranes together with glue, were attached to the top and bottom loading platens (as indicated in Fig. 2 (a)) to avoid mechanical noise caused by the loading system. Thereafter, the particle was placed between two platens, and the top platen was set to move downward at a displacement rate of 0.2 mm/min. Transducers of a load cell and an external displacement transducer were installed to measure the axial loading force and displacement respectively.

2.2. AE measurement system

A high-performance AE measurement system with high sensitivity, high SNR (signal to noise ratio), broadband working frequency and high sampling rate was used to continuously monitor the fracturing process. Seven piezo-ceramics type AE sensors, produced by Fuji Ceramics Corporation: M304A, were used. These AE sensors, which have a working frequency of 10 kHz–5 MHz (resonant frequency at 300 kHz) and a sensitivity of 115 ± 3 dB (ref. 0 dB = 1 V/m/s), were designed to locate at the top and middle height of the bottom platen, as shown in Fig. 2 (a). The captured signals were further amplified by two amplifiers of a built-in preamplifier (with a gain of 20 ± 2 dB) and a main amplifier (with a gain of 53 ± 3 dB). A data logger “PXIe-6366

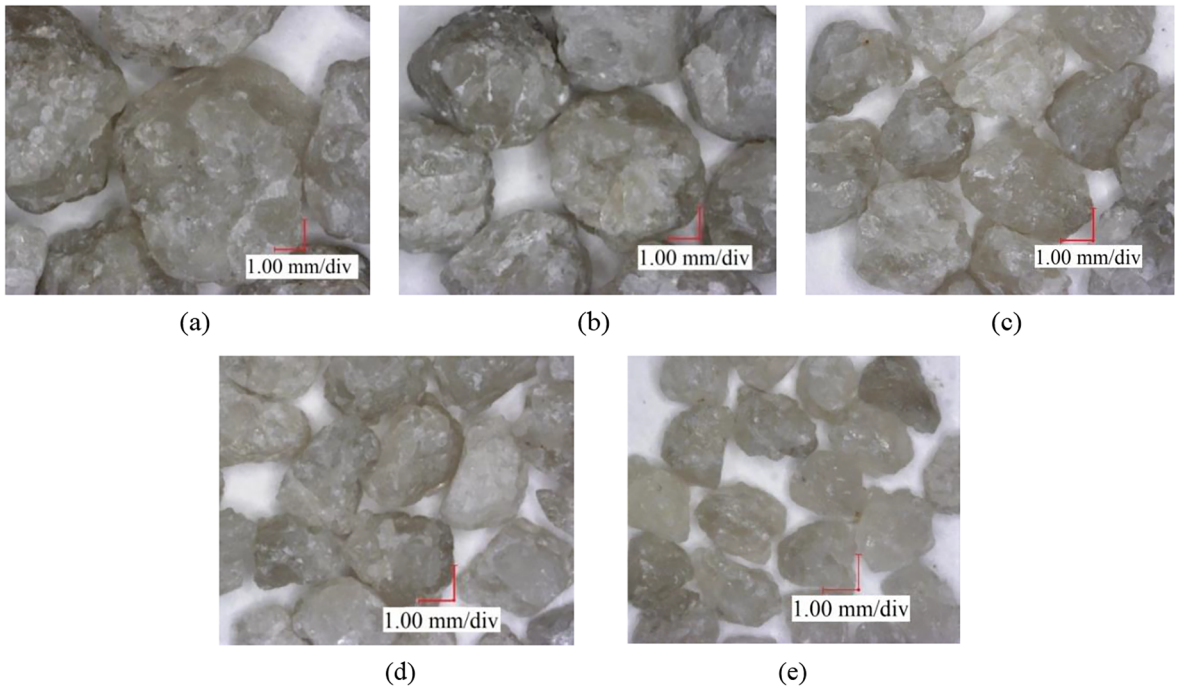

Fig. 1. Optical images of silica sand particles with five different sizes in case of (a) Silica # 1, (b) Silica # 2, (c) Silica # 3, (d) Silica # 4, (e) Silica # 5.

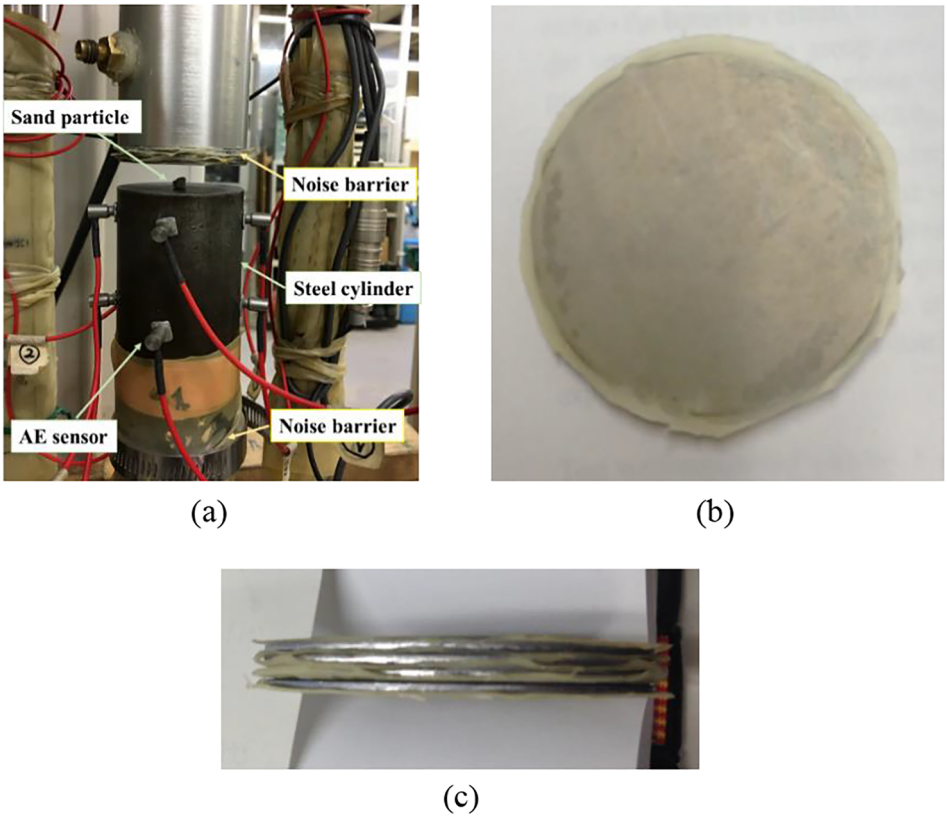

Fig. 2. Schematic illustration of (a) experimental apparatus, (b) front view of noise barriers, and (c) side view of noise barriers.

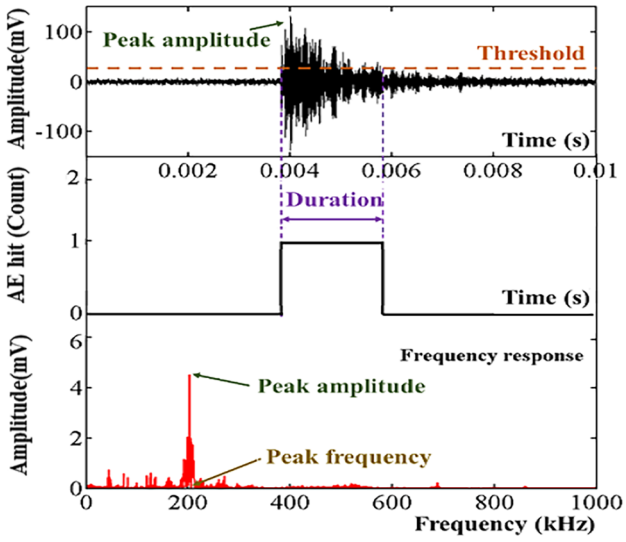

Fig. 3. Typical AE waveform and involved parameters generated from the process of single particle compression.

data logger" (manufactured by National Instruments Corporation) with a maximum analogue input sampling rate of 2 MS/s was used. With this setup, a sampling rate of 2 MS/s was adopted to continuously record the original AE signal without any signal pre-processing.

A typical AE waveform, as well as the involved parameters, is displayed in Fig. 3. In order to discriminate the AE signal, a threshold of 29.54 dB (ref. 0 dB = 1 mV/m/s in this work) based on the voltage level caused by electrical and ambient noise (around 20 dB, ref. 0 dB = 1 mV/m/s) was set first. Once a signal exceeds the threshold, an AE signal is identified and defined as one hit. To analyze the frequency characteristic of detected AE signals, Fast Fourier Transformation (FFT) method was used to convert the signal from the time domain into the frequency domain, and the frequency component with peak amplitude in the spectrum is regarded as the peak frequency. In this work, both parameters of AE hit rate (i.e. the accumulation of AE hits in 1 s) and peak frequency were analyzed for further interpretation.

3. Testing results

3.1. Load-displacement relations during single particle compression

Fig. 4 shows the typical load-displacement relations for single particle compression tests under different sizes. It can be seen that the stiffness, i.e. the tangent modulus of the linear part, is seen similar to each other regardless of different sizes. Besides, the evolution of load-displacement relations, where the load increases rapidly to a distinct peak value followed by a transient plummeting, behaves similarly to the stress-strain evolution of brittle rocks subjected to compression. Generally, the failure process of rock materials is divided into five stages in terms of stress-strain and AE hit rate-strain relations [22,23]. Considering that sand particle is in a sense belongs to rock material, analogously, we also divide its fracturing process leading up to failure into five stages in terms of (I) adjustment stage, (II) linear elastic deformation stage, (III) micro-crack initiation and stable growth stage, (IV) unstable micro-crack growth stage, and (V) failure stage. A similar division of five stages for single particle compression was also suggested by Cavarretta and O'Sullivan [24]. It should be noted that due to the intrinsic difference in the appearance configuration (e.g. shapes and sizes) and/or inner defects, etc., each particle has its own mechanical characteristic. The five stages might not be linearly sequential, and the particle does not necessarily undergo through the whole five fracturing stages. Some stages may overlap partially or entirely, and one or some stage(s) may shrink or even disappear along its way to failure.

Nevertheless, to fully interpret each stage, one of the test results of Silica #2, where five stages are clearly demonstrated, is taken as an

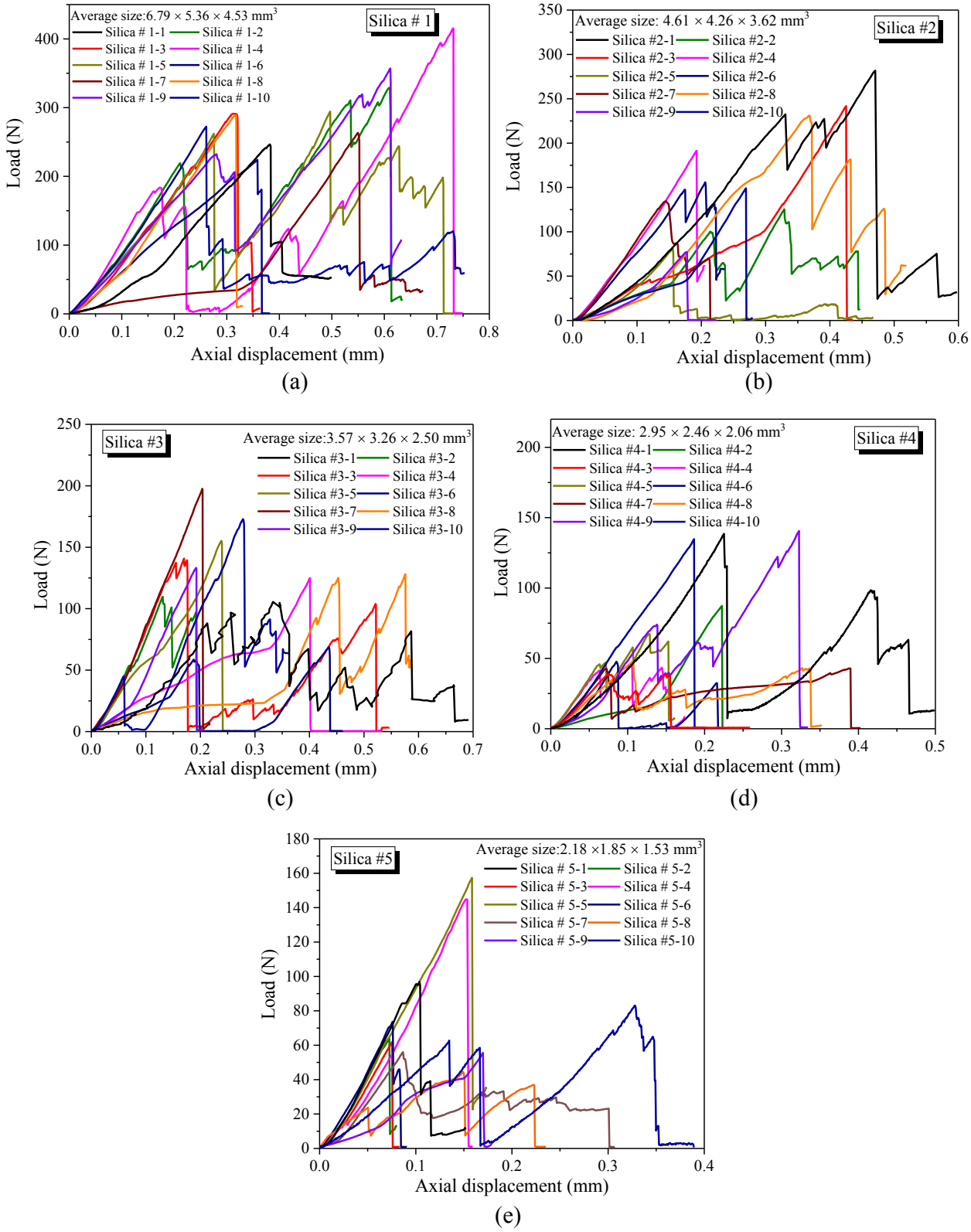

Fig. 4. Typical load-displacement relations during single particle compression tests of silica sand particles with five different sizes of (a) Silica # 1, (b) Silica # 2, (c) Silica # 3, (d) Silica # 4, and (e) Silica #5.

illustration, as shown in Fig. 5. In the adjustment stage (I), the particle accommodates itself with the loading platens in terms of particle rotation and sliding. The stiffness increases gradually and the load-displacement curve presents as a concave shape. As the load increases, the particle enters into the linear elastic zone and the stiffness reaches its maximum. In rock mechanics, this linear elastic zone is usually divided into two stages of (II) linear elastic deformation stage and (III) crack initiation and stable growth stage, demarcated by the inflexion point at its volumetric strain curve [23]. In this work, since the volumetric strain is un-measurable, the demarcation point is hard to be determined

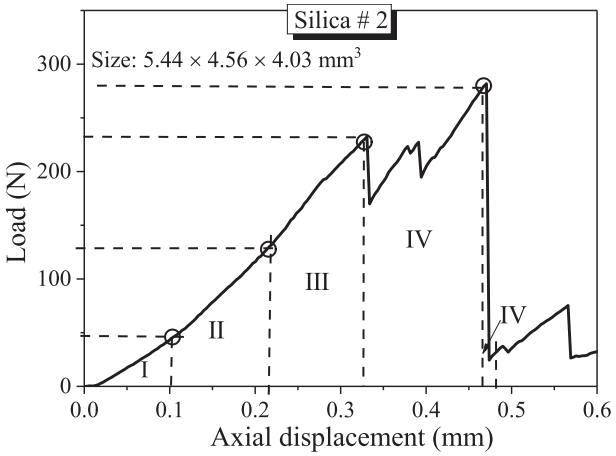

Fig. 5. Example (silica #2) of five divided stages in the load-displacement curve during the process of single particle compression.

in the load-displacement curve. Nevertheless, it might be determined by the AE characteristic, as will be illustrated in Section 3.2. In stage II, the particle undergoes elastic deformation. In this stage, the stress is not yet high enough to initiate new, stress-induced microcracks [25], while it might be high enough to cause asperity chipping and abrasion. As the particle enters into the stage III, the increasing load enables the new, stress-induced microcracks to subsequently initiate and stably grow with compression. As the particle approaches the failure time (IV), microcracks develop and coalesce rapidly, and even some weak corners are likely to break off, causing the load to increase with fluctuation. The particle finally fails by splitting (e.g. Silica # 2) or chipping (e.g. Silica # 3)) in stage V due to the fully coalescent of microcracks, accompanying by the plummeting of the loading force. Thereafter, the broken piece split from the parent particle lies in the loading platen for further fragmentation, demonstrating as the subsequent ups and downs in load.

3.2. AE characteristics during single particle compression

Various AE parameters (e.g. AE hit rate, amplitude, frequency characteristic, source location, etc.) have been utilized to characterize the deterioration and failure mechanism of stressed material. Particularly, the parameter of AE hit rate is recognized capable of continuously disclosing the intensity of cracking or fracturing behaviors leading up to failure [12,13]. While AE frequency response could distinguish different modes of source mechanisms, e.g. micro-defect closure and opening against cracking, tensile cracking against shear cracking, particle sliding against collisions, etc. [25–27]. In this work, acoustic emissions are considered mainly generating from the micro-mechanical behaviors including particle readjustment (e.g. particle sliding), asperity abrasion, and microcracking. To indicate the deterioration intensity and distinguish different modes of micro-mechanical behaviors during fracturing, the AE hit rate and peak frequency were analyzed respectively. Since all AE sensors demonstrate the same result, for a brief, only the sensor connected to channel 1 would be illustrated in the following section.

3.2.1. Evolution of AE hit rate during single particle compression

Fig. 6 presents the typical AE hit rate derived from the tested particles with various sizes. It is observed that regardless of different sizes, the evolution of the AE hit rate during the fracturing process shares a similar tendency. Take one of the testing results of Silica #2 as an example (Fig. 6 (b)). The particle is initially featured by a flurry of AE hits in the adjustment stage (I) due probably to particle rotation/sliding. While the AE hit rate tends to die down as the particle enters into the stage II. This might not be surprised because acoustic waves are strongly dependent on irreversible (non-elastic) deformations. However, it should be noted that the load in this stage might be high enough to cause surface asperities to abrade, and hence generates a few acoustic emissions [25]. Thereafter, AE hit rate restarts to increase in the latter linear compression stages (III), followed by a rapid increase in the impending failure stage (IV). It seems that although the particle still demonstrates as a linear deformation manner in stage III, its internal micro-mechanical behaviors might be different from stage II. One of the possible explanations would be the initiation and evolution of microcracking with the increasing load. Finally, an extremely rapid rise of AE hit rate is observed as immediately as the particle is split (V). The similar tendency, though involved with different materials, was also reported by Ohnaka and Mogi [25], He et al. [28] and Mao and Towhata [16]. Since sandy particles are stochastic, particles with different appearance configuration and inner defects will not give exactly the same fracturing process. Such differences are also well featured by the characteristic of AE hit rate. For example particles which are fragile and failed by chipping-type are more likely to break and, hence, generate sufficient AE activities (e.g. Silica # 3).

Note that a precursory anomaly of AE hit rate — the rapid increase at the impending failure stage, is found additionally consistent with previous observations conducted in rock materials by Kranz [29] and Lei et al. [12]. Such precursory behavior in AE is stated closely related to the microcracking initiation and coalescence, and hence, could be regarded as an omen for early warning against the instability of tested materials. Details will be also discussed in Section 4.

Another anomaly is that after the catastrophic failure (i.e. particle splitting or chipping), the remaining broken piece, which continuously acts as a “new particle” for further fragmentation, becomes more emissive even under an extremely low load level. It seems that the “new particle” might have been covered with many “injuries” (i.e. microcracks) after it suffering from the prehistory of catastrophic damage. This demonstrates the significant effect of “prehistory of failure” on the mechanical behavior of sandy particles, although such physical insights might be sometimes difficult to be induced from the conventional load-deformation relation (e.g. Silica # 4 and Silica # 5). It seems that the evolution of AE hit rate could more sensitively reflect such effect, compared with the conventional load-displacement manifestation.

3.2.2. Frequency characteristics of AE during single particle compression

Fig. 7 shows four typical AE waveforms of Silica # 2, as well as their corresponding frequency response, during the fracturing process. Each AE waveform contains broadband frequency components with its peak frequency ranging from 40 kHz to 500 kHz, indicating that different modes of micro-mechanical behaviors might be occurred during fracturing.

Fig. 8 further shows the peak frequency response of all AE waveforms generated from the whole fracturing process, along with the corresponding load–displacement relation. It is found that despite of different particle sizes, the overall evolution of AE peak frequency during fracturing is seen similar. Again, one of the results of silica # 2 was taken as an illustration (Fig. 8 (b)). The flurry of AE hits generated during the particle readjustment (e.g. particle sliding) in stage (I) is found to be predominated by low frequency (abbreviated as LF thereafter) AE components at around 50 kHz. While the initial linear load-displacement part, where AE activities are inactive, is featured by not only a few LF components but also a few medium-high frequency (abbreviated as MHF thereafter) components up to 200 kHz. Considering that the stress in this stage might be high enough to cause asperity abrasion, these behaviors are, therefore, considered contributing to generating such MHF AEs. As compression progresses, the re-increase of AE hit rate in the late linear part is featured by relatively broadband frequency AEs. Particularly, high-frequency (abbreviated as HF thereafter) AEs with peak frequency ranging from 200 to 600 kHz are observed initiating in this stage. Thereafter, HF components (200–600 kHz) increases more rapidly as the particle approaches failure (IV), especially when some weak corners are broken off. Finally, the

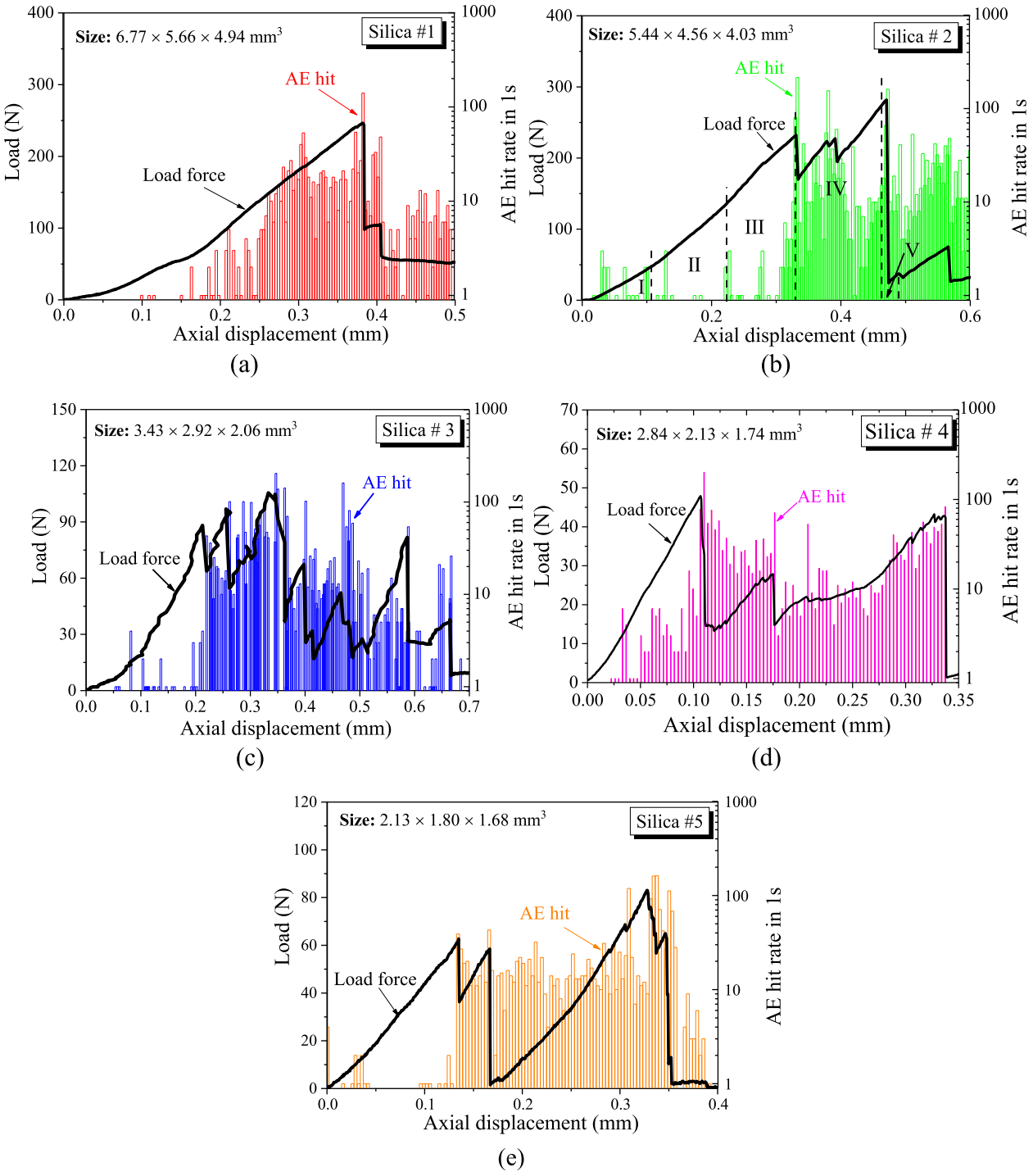

Fig. 6. Evolutions of AE hit rate during the fracturing process of single particle compression with different particle sizes of (a) Silica # 1, (b) Silica # 2, (c) Silica # 3, (d) Silica # 4, and (e) Silica # 5.

extremely high rate of acoustic emissions generated in the failure stage is featured by broadband frequency components up to 600 kHz. It seems that the initiation and the rapid increase of HF components are closely related to the initiation and evolution of microcracking, in which the moment that HF components initiated might be regarded as the demarcation point for stage II and stage III, and also might be used as an omen for early warning the microcracking behavior leading up to failure as well.

Note that, for large particles such as silica #1, the initially generated AEs in stage I is predominated by only LF components at around 50 kHz. With the decrease of particle sizes, the AE generated at the beginning of compression stage tends to be predominated by not only LF components but also MHF components up to around 200 kHz. Typical results are those obtained from Silica # 4 and Silica #5. One of the possible reasons is that a given load applied on a smaller contact area of smaller particles yields a higher contact stress, which could easily cause asperities to abrade; and consequently, generate higher frequency components.

It should be also noted that LF components, and even MHF components, are observed appearing throughout almost the entire compression history, indicating that micro-mechanical behaviors of particle readjustment and asperity abrasion might occur throughout almost the

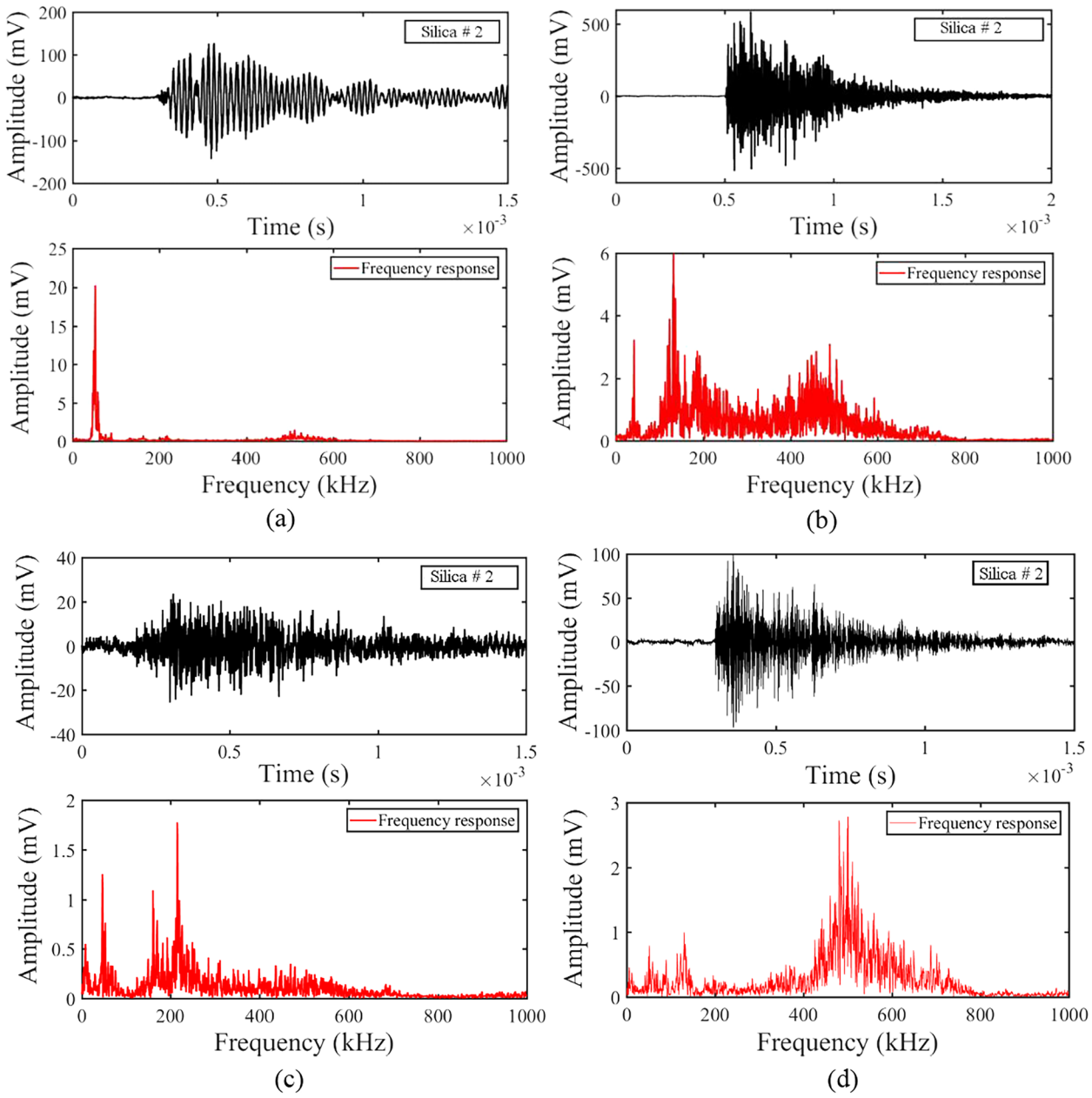

Fig. 7. Typical AE waveforms and their corresponding frequency characteristics obtained from Silica # 2 subjected to single particle compression.

entire loading history. These phenomena are convincible because when breakage occurs, interactions in terms of sliding and rotation of fractured pieces along the contacted rough surface would be inevitable, as well as the asperity abrasion between the particle and the loading platen [30]. As a consequence, both LF and MHF components emerge as co-products along with the entire compression history.

4. Discussion and summary

The present experimental result illustrates that, regardless of different particle appearance configurations (i.e. size, shape), the fracturing process of the sandy particle could be highly featured by AE characteristics in terms of AE hit rate and frequency characteristic. The intensity of micro-mechanical behaviors could be featured by AE hit rate, while the mode of different micro-mechanical behaviors associating with particle readjustment, asperity abrasion, and microcracking could be featured by AE frequency characteristics. Main features of micro-mechanical behaviors and corresponding AE characteristics during the fracturing process of single particle compression are summarized in Table 2.

The generation of LF (at around 50 kHz) components throughout the whole testing is interpreted resulting from particle readjustment (e.g. particle sliding and rotating). Such consideration is validated by previous studies [16,27,15] where particle sliding behaviors (i.e. particle-to-particle sliding or particle-to-metal sliding) were simulated and revealed highly featured by low-frequency AE components up to 80 kHz.

On the other hand, the initiation and rapid increase of HF components (200–600 kHz) occurred at the impending failure stage indicate the initiation and evolution of microcracking, which might be regarded as omens for instability warning of sandy particles. Previous studies [e.g. [25,12,31–33]] conducted in rock, concrete and sandstone materials have also proved that cracking and fracturing generate higher frequency AEs. For instance, Read et al. [32] found that cracking events of porous rocks subjected to triaxial compression would generate AEs with frequency components ranged within 100–600 kHz. Kato et al. [33] reported AEs originated from shear rupture of granite samples

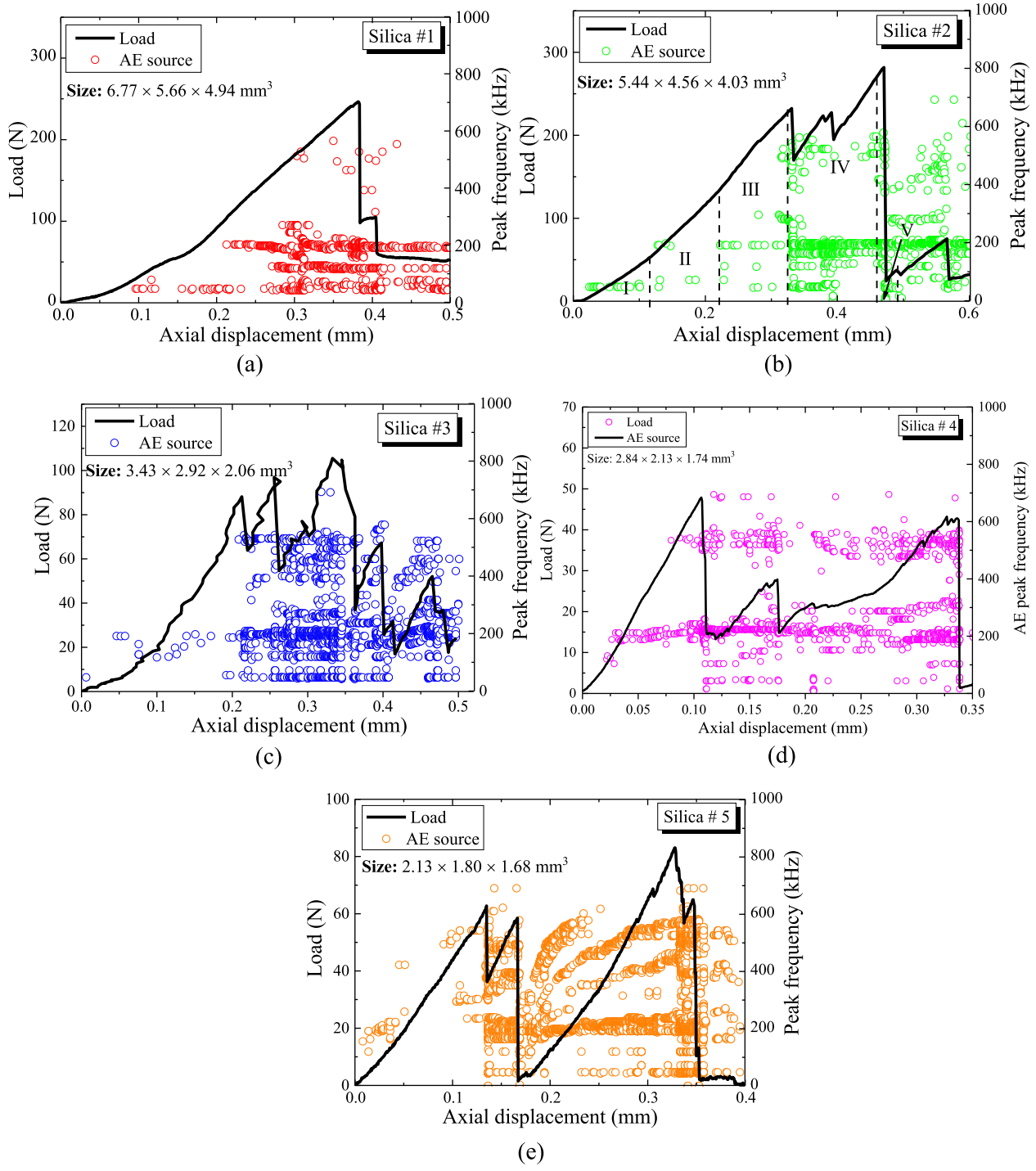

Fig. 8. AE frequency characteristics during the fracturing process of single particle compression with different particle sizes of (a) silica # 1, (b) Silica # 2, (c) Silica # 3, (d) Silica # 4, (e) Silica # 5.

Table 2
Main features of AE characteristics during single particle compression process.

Stage	Micro-mechanical behavior	AE hit rate	Frequency characteristics
I	Particle readjustment (sliding and rotation)	A flurry of AEs	LF AEs at around 50 kHz
II	Asperity abrasion	Inactive AEs	A few LF and MHF components up to 200 kHz
III	Initiation of new, stress-induced microcracks	Re-increase of AE hit rate	Initiation of HF AEs (200–600 kHz)
IV	Unstable growth of microcracks	Rapid increase of AE hit rate	Rapid increase of HF AEs (200–600 kHz)
V	Coalescent of microcracks (particle splitting or chipping)	Extremely high level of AE hit rate	Board band frequency AEs up to 600 kHz

*Note: LF refers to low frequency, MHF refers to medium high frequency, and HF refers to high frequency.

were dominated by frequency components of 200 kHz–1 MHz. These results coincide very well with the present result on sandy particles.

In addition to microcracking initiation and evolution, it should be noted that the micro-mechanical behavior of asperity abrasion is prone to generate medium-high AE components ranged within 100–200 kHz. Such a phenomenon is plausible since asperity abrasion is indeed involved with the mechanical break off of asperities and is physically similar to particle crushing behavior. Similarly, Ohnaka and Mogi [25] and Kato et al. [33] also have argued that the rupturing of healed preexisted crack or asperities shearing on the rock surface under a higher stress level would contribute to the generation of medium-high frequency AEs (100–400 kHz).

Based on the above results, it is understood that particle readjustment (particle sliding and rotating) is closely related to lower frequency AE components, while particle breakage behaviors in terms of asperity abrasion and microcracking are prone to generate higher frequency components. To this end, a frequency-based demarcation method could be therefore suggested to discriminate different modes of micro-mechanical behaviors in terms of particle readjustment (say, below 100 kHz), asperity abrasion (say, 100–200 kHz) and microcracking (say, 200–600 kHz) for granular particles subjected to compression. The further application of present results in stressed granular assemblages is expected to continuously evaluate the intensity and mode of particle interactions during laboratory testing.

5. Concluding remarks

In this work, a series of single particle compression tests incorporating with AE technique were conducted on silica sand particles with five different sizes under dry condition. The fracturing process was analyzed and summarized by correlating load-displacement relations with AE characteristics (i.e. AE hit rate and frequency characteristics). Some insights could be offered as follow.

(1) Regardless of different particle sizes, the fracturing process of a single sand particle subjected to compression could be highly featured by AE characteristics, where AE hit rate and AE peak frequency response could highly feature the intensity and mode of micro-mechanical behaviors, respectively.
(2) The initiation and rapid increase of high frequency AE components (200–700 kHz), as well as the corresponding re-increase and rapid increase of AE hit rate, are closely related to the initiation and evolution of microcracking, which might be used as omens for early warning the impending failure of stressed particles.
(3) The broken piece split from the parent particle becomes more emissive even under a low load level, showing a significant effect of “prehistory of failure” on the mechanical behavior of sandy particles. The result suggests that AE technique could more sensitively reflect such effect, compared with conventional load-displacement manifestation.
(4) The generation of lower frequency AE components (below 100 kHz), medium-high frequency AE components (100–200 kHz) and high-frequency components (200–700 kHz) are considered resulting from different modes of micro-mechanical behaviors of particle readjustment, asperity abrasion, and microcracking, respectively. A frequency-based demarcation method is therefore suggested and expected to be employed in stressed granular assemblages to continuously evaluate the intensity and mode of particle interactions.

Acknowledgement

This study was financially supported by the National Natural Science Foundation of China (Grant No. 41602302), JSPS KAKENHI (Grant No. JP16K14301), Shanghai Sailing Program (Grant No. 18YF1424000) and the China Scholarship Council (Grant No. 201506260190).

Appendix A. Supplementary material

Supplementary data to this article can be found online at https://doi.org/10.1016/j.ultras.2019.105962.

References

[1] P.V. Lade, J. Nam, C.D. Liggio, Effects of Particle crushing in stress drop-relaxation experiments on crushed coral sand, J. Geotech. Geoenviron. Eng. 136 (3) (2010) 500–509, https://doi.org/10.1061/(ASCE)GT.1943-5606.0000212.
[2] V. Bandini, M.R. Coop, the influence of particle breakage on the location of the critical state line of sands, Soils Found. 51 (4) (2011) 591–600, https://doi.org/10.3208/sandf.51.591.
[3] F. Yu, Particle breakage and the drained shear behavior of sands, Int. J. Geomech. 17 (8) (2017) 04017041, https://doi.org/10.1061/(ASCE)GM.1943-5622.0000919.
[4] G.R. McDowell, A. Amon, The application of Weibull statistics to the fracture of soil particles, Soils Found. 40, N0.5 (2000) 133–141.
[5] I. Cavarretta, M. Coop, C. O’Sullivan, The influence of particle characteristics on the behaviour of coarse grained soils, Géotechnique 60 (6) (2010) 413–423, https://doi.org/10.1680/geot.2010.60.6.413.
[6] B. Zhao, J. Wang, M.R. Coop, G. Viggiani, M. Jiang, An investigation of single sand particle fracture using X-ray micro-tomography, Géotechnique 65 (8) (2015) 625–641, https://doi.org/10.1680/geot.4.P.157.
[7] W. Wang, M.R. Coop, An investigation of breakage behaviour of single sand particles using a high-speed microscope camera, Géotechnique 66 (12) (2016) 984–998, https://doi.org/10.1680/jgeot.15.P.247.
[8] ASTM E1316-14e. (2015) Standard terminology for nondestructive examinations. American society for testing and materials.
[9] A. Ebrahimkhanlou, S. Salamone, Acoustic emission source localization in thin metallic plates: A single-sensor approach based on multimodal edge reflections, Ultrasonics 78 (2017) 134–145, https://doi.org/10.1016/j.ultras.2017.03.006.
[10] A. Ebrahimkhanlou, S. Salamone, A probabilistic framework for single-sensor acoustic emission source localization in thin metallic plates, Smart Mater. Struct. 26 (2017) 095026, , https://doi.org/10.1088/1361-665X/aa78de.
[11] A. Ebrahimkhanlou, S. Salamone, Single-sensor acoustic emission source localization in plate-like structures using deep learning, Aerospace 5 (2) (2018) 50, https://doi.org/10.3390/aerospace5020050.
[12] X. Lei, K. Masuda, O. Nishizawa, L. Jouniaux, L. Liu, W. Ma, K. Kusunose, Detailed analysis of acoustic emission activity during catastrophic fracture of faults in rock, J. Struct. Geol. 26 (2) (2004) 247–258, https://doi.org/10.1016/S0191-8141(03)00095-6.
[13] R. Yuan, B. Shi, Acoustic emission activity in directly tensile test on marble specimens and its tensile damage constitutive model, Int. J. Coal Sci. Technol. 5 (3) (2018) 295–304, https://doi.org/10.1007/s40789-018-0215-4.
[14] X. Liu, L. Wu, Y. Zhang, Z. Liang, X. Yao, P. Liang, Frequency properties of acoustic emissions from the dry and saturated rock, Environ. Earth Sci. 78 (3) (2019) 67, https://doi.org/10.1007/s12665-019-8058-x.
[15] S. Dagois-Bohy, S. Ngo, S.C. du Pont, S. Douady, Laboratory singing sand avalanches, Ultrasonics 50 (2) (2010) 127–132, https://doi.org/10.1016/j.ultras.2009.09.027.
[16] W. Mao, I. Towhata, Monitoring of single-particle fragmentation process under static loading using acoustic emission, Appl. Acoust. 94 (2015) 39–45, https://doi.org/10.1016/j.apacoust.2015.02.007.
[17] N. Dixon, M.P. Spriggs, A. Smith, P. Meldrum, E. Haslam, Quantification of reactivated landslide behaviour using acoustic emission monitoring, Landslides 12 (3) (2015) 549–560, https://doi.org/10.1007/s10346-014-0491-z.
[18] A. Smith, N. Dixon, G.J. Fowmes, Early detection of first-time slope failures using acoustic emission measurements: large-scale physical modelling, Géotechnique 67 (2) (2017) 138–152, https://doi.org/10.1680/jgeot.15.P.200.
[19] S. Luo, A. Diambra, E. Ibraim, Application of acoustic emission on crushing monitoring of individual soil particles in uniaxial compression test, 32nd European Conference on Acoustic Emission Testing Prague, Czech Republic, September 07-09 2016, 2016, pp. 305–314.
[20] S. Luo, A. Diambra, E. Ibraim, Particle crushing: passive detection, 1st IMEKO TC-4 International Workshop on Metrology for Geotechnics Benevento, Italy, March 17-18, (2016).
[21] E. Ibraim, S. Luo, A. Diambra, Particle soil crushing: passive detection and interpretation, Proceedings of the 19th International Conference on Soil Mechanics and Geotechnical Engineering. Seoul, 2017, pp. 389–392.
[22] R.E. Goodman, Introduction to rock mechanic, Wiley, New York, 1989.
[23] E. Eberhardt, D. Stead, B. Stimpson, R.S. Read, Identifying crack initiation and propagation thresholds in brittle rock, Can. Geotech. J. 35 (2) (1998) 222–233 https://doi:10.1139/t97-091.
[24] I. Cavarretta, C. O’Sullivan, The mechanics of rigid irregular particles subject to uniaxial compression, Géotechnique 62 (8) (2012) 681–692, https://doi.org/10.1680/geot.10.P.102.
[25] M. Ohnaka, K. Mogi, Frequency characteristics of acoustic emission in rocks under uniaxial compression and its relation to the fracturing process to failure, J.

Geophys. Res. 87 (B5) (1982) 3873–3884, https://doi.org/10.1029/JB087iB05p03873.
[26] K. Ohno, M. Ohtsu, Crack classification in concrete based on acoustic emission, Constr. Build. Mater. 24 (12) (2010) 2339–2346, https://doi.org/10.1016/j.conbuildmat.2010.05.004.
[27] G. Michlmayr, D. Or, Mechanisms for acoustic emissions generation during granular shearing, Granular Matter 16 (5) (2014) 627–640, https://doi.org/10.1007/s10035-014-0516-2.
[28] M.C. He, J.L. Miao, J.L. Feng, Rock burst process of limestone and its acoustic emission characteristics under true-triaxial unloading conditions, Int. J. Rock Mech. Min. Sci. 47 (2) (2010) 286–298, https://doi.org/10.1016/j.ijrmms.2009.09.003.
[29] R.L. Kranz, Crack growth and development during creep of barre granite, Int. J. Rock Mech. Min. 16 (1) (1979) 23–35, https://doi.org/10.1016/0148-9062(79)90772-1.
[30] I. Einav, Breakage mechanics-Part II: Modelling granular materials, J. Mech. Phys. Solids 55 (6) (2007) 1298–1320, https://doi.org/10.1016/j.jmps.2006.11.004.
[31] C.H. Sondergeld, L.H. Estey, Acoustic emission study of microfracturing during the cyclic loading of Westerly granite, J. Geophys. Res. 86 (B4) (1981) 2915–2924, https://doi.org/10.1029/JB086iB04p02915.
[32] M.D. Read, M.R. Ayling, P.G. Meredith, S.A.F. Murrell, Microcracking during triaxial deformation of porous rocks monitored by changes in rock physical properties, II. Pore volumometry and acoustic emission measurements on water-saturated rocks, Tectonophysics 245 (34) (1995) 223–236, https://doi.org/10.1016/0040-1951(94)00236-3.
[33] N. Kato, K. Yamamoto, T. Hirasawa, Microfracture processes in the breakdown zone during dynamic shear rupture inferred from laboratory observation of near-fault high-frequency strong motion, Pure Appl. Geophys. Pageoph. 142 (3–4) (1994) 713–734, https://doi.org/10.1007/BF00876061.